Biochimica et Biophysica Acta 1837 (2014) 1981–1988

Contents lists available at ScienceDirect

Biochimica et Biophysica Acta

journal homepage: www.elsevier.com/locate/bbabio

Disturbed excitation energy transfer in *Arabidopsis thaliana* mutants lacking minor antenna complexes of photosystem II

Luca Dall'Osto [a,1], Caner Ünlü [b,1], Stefano Cazzaniga [a], Herbert van Amerongen [b,c,*]

[a] Dipartimento di Biotecnologie, Università di Verona, 37134 Verona, Italy
[b] Laboratory of Biophysics, Wageningen University, 6703 HA Wageningen, The Netherlands
[c] MicroSpectroscopy Centre, Wageningen University, 6703 HA Wageningen, The Netherlands

ARTICLE INFO

Article history:
Received 21 May 2014
Received in revised form 28 September 2014
Accepted 29 September 2014
Available online 5 October 2014

Keywords:
Photosynthesis
Light-harvesting complex
Photosystem II
Time-resolved fluorescence spectroscopy
Thylakoid membrane

ABSTRACT

Minor light-harvesting complexes (Lhcs) CP24, CP26 and CP29 occupy a position in photosystem II (PSII) of plants between the major light-harvesting complexes LHCII and the PSII core subunits. Lack of minor Lhcs *in vivo* causes impairment of PSII organization, and negatively affects electron transport rates and photoprotection capacity. Here we used picosecond-fluorescence spectroscopy to study excitation-energy transfer (EET) in thylakoid membranes isolated from *Arabidopsis thaliana* wild-type plants and knockout lines depleted of either two (koCP26/24 and koCP29/24) or all minor Lhcs (NoM). In the absence of all minor Lhcs, the functional connection of LHCII to the PSII cores appears to be seriously impaired whereas the "disconnected" LHCII is substantially quenched. For both double knock-out mutants, excitation trapping in PSII is faster than in NoM thylakoids but slower than in WT thylakoids. In NoM thylakoids, the loss of all minor Lhcs is accompanied by an over-accumulation of LHCII, suggesting a compensating response to the reduced trapping efficiency in limiting light, which leads to a photosynthetic phenotype resembling that of low-light-acclimated plants. Finally, fluorescence kinetics and biochemical results show that the missing minor complexes are not replaced by other Lhcs, implying that they are unique among the antenna subunits and crucial for the functioning and macro-organization of PSII.

1. Introduction

Oxygenic photosynthesis is performed in the chloroplast by a series of reactions which transform sunlight energy into chemical energy [1]. Absorption of light, excitation energy transfer (EET) and electron transfer are the primary events of the photosynthetic light phase and take place in photosystems (PS) I and II [2–10]. PSII is a large supramolecular pigment–protein complex located in the thylakoid membranes of plants, algae and cyanobacteria. Its reaction center (RC) consists of several subunits carrying the cofactors for electron transport and forms, together with the proteins CP43 and CP47 a so-called core complex [11,12]. Core complexes form dimers (C_2), which bind a system of nuclear-encoded light-harvesting proteins (Lhcbs): CP29 and CP26 are monomeric antennae located in close connection to the core, and seem to mediate the binding of an LHCII trimer (the major antenna complex of PSII) called LHCII-S (strongly bound), thus forming the basic PSII supercomplex structure C_2S_2 [13]. Moreover, in higher plants another monomeric subunit (CP24) and one more trimeric LHCII (LHCII-M, "moderately" bound) bind the PSII core to extend the light-harvesting capacity of the supercomplex (called $C_2S_2M_2$). Besides light harvesting, the outer antenna of PSII plays a crucial role in photoprotective and regulatory mechanisms such as limiting the level of Chl triplet states [14–16], scavenging of reactive oxygen species [17] and activating non-radiative de-excitation pathways [18].

Excitations are used to induce primary charge separation (CS) within the RC, after which electrons are transferred in succession to the acceptors Q_A and Q_B, while the oxidizing equivalents in the Mn cluster are used to catalyze water splitting [1]. The quantum efficiency of CS depends on the rate constants of different molecular events, namely 1) EET from the outer antenna to the RC; 2) CS and charge recombination; 3) secondary electron transfer to Q_A, and 4) relaxation processes, such as intersystem crossing, internal conversion and fluorescence emission [19].

Among the antenna complexes of PSII, monomeric Lhcs CP24, CP26 and CP29 are of particular interest, because the location of these complexes in between LHCII and the RC makes them crucial for facilitating EET from LHCII, forming the major part of the antenna system, to the core subunits, although it seems that also direct EET

* Corresponding author at: Laboratory of Biophysics, Wageningen University, Dreijenlaan 3, 6703 HA Wageningen, The Netherlands. Tel.: +31 317482634; fax: +31 317482725.
E-mail address: herbert.vanamerongen@wur.nl (H. van Amerongen).
[1] Both authors equally contributed to this work.

http://dx.doi.org/10.1016/j.bbabio.2014.09.011

from LHCII-S to the core is possible [20,21]. Indeed, depletion of specific monomeric Lhcs *in vivo* was shown to impair the organization of photosynthetic complexes within grana partitions, and to negatively affect electron transport rates and photoprotection capacity [22]. Evidence that these gene products have been conserved over at least 350 million years of evolution [23] strongly indicates that each complex has a specific role in the PSII function over the highly variable conditions of the natural environment.

CS in the reaction centers of PSI and PSII occurs within tens to hundreds of picoseconds (ps) after light absorption. A great challenge in studying EET and charge separation in thylakoid membranes is to disentangle the kinetics related to both photosystems. Broess et al. [24] and Caffari et al. [20] recently provided a more detailed picture of EET in PSII membranes and supercomplexes of plants while van Oort et al. [25] investigated EET in entire thylakoids of WT and mutant *Arabidopsis* with the use of ps-fluorescence spectroscopy, using different combinations of excitation/detection wavelengths, in order to distinguish PSI and PSII kinetics. The exciton/radical-pair-equilibrium (ERPE) model has often been used to describe the kinetics of EET in PSII preparations with open RCs, *i.e.* with the electron acceptor Q_A fully oxidized [26,27]. This model assumes that EET to the RC is too fast to contribute substantially to the charge separation time [26]. To provide a more accurate description for grana-enriched membranes, the ERPE model was extended after analyzing ps-fluorescence measurements using different excitation wavelengths and applying a coarse-grained model to determine the excitation migration time to the RC [24]. Comparison of the fluorescence kinetics obtained for 412 nm (more excitations in the core) and 484 nm excitation (more excitations in the outer antenna), led to the conclusion that the average migration time of an excitation toward the RC contributes 20–25% to the average trapping time in PSII membranes and around 50% in full thylakoid membranes [25,28,29] and the overall migration time to the RC is around 150 ps in WT thylakoids, four times longer than for grana-enriched membranes [24] which is likely due to additional antenna complexes that are less well connected to the PSII RC [21,25,28–30] and that are lost during preparation of grana membranes [21]. Recently, also models were presented that assume excitation trapping the time of which is entirely dominated by migration of excitations to the RC [31,32].

Recent studies on EET dynamics focused on the behavior of specific pigment–protein complexes that constitute either PSI or PSII [33–35]. Reverse genetic approaches in model organisms such as *Arabidopsis thaliana* allowed to isolate knock-out lines devoid of specific components of PSII [36,37] and have been instrumental in order to dissect the function of each subunit *in vivo*. Hopefully, applying time-resolved spectroscopy on thylakoid membranes of different composition can provide new knowledge on the primary events of the light phase at the molecular level.

In this work, thylakoid membranes of *A. thaliana* have been studied with time-resolved fluorescence spectroscopy using different combinations of excitation and detection wavelengths, in order to (partly) separate PSI and PSII/LHCII contributions. In particular, PSII/LHCII fluorescence decay kinetics have been measured on thylakoids isolated from wild-type *Arabidopsis*, from the double knock-out mutants koCP26/24 and koCP29/24, and from a mutant depleted of all minor antennae (NoM). The main goal of this study was to investigate how the depletion of specific Lhcs affects the excitation- and electron-transfer parameters of PSII. In the absence of all minor Lhcs of PSII, the functional connection between LHCII from the PSII cores appears to be strongly impaired and LHCII is substantially quenched which is probably related to the fact that the NoM plants are strongly hampered in their growth as compared to WT plants. For double knock-out mutants, the outer antenna is better connected to the PSII core and the corresponding plants also grow significantly better than the NoM plants.

2. Materials and methods

2.1. Plant material and growth conditions

WT plants of *A. thaliana* ecotype Col-0 and mutants *koLhcb4.1*, *koLhcb4.2*, *koLhcb5* and *koLhcb6* were obtained as previously described [36,37]. Multiple mutants *koLhcb5 koLhcb6* (koCP26/24), *koLhcb4.1 koLhcb4.2* (koCP29/24) and *koLhcb4.1 koLhcb4.2 koLhcb5* (NoM) were isolated by crossing single mutant plants and by selecting the progeny through immunoblotting, using antibodies specific for the different Lhcb subunits. Double mutant *koLhcb4.1 koLhcb4.2* is devoid of both CP29 and CP24 minor antennae, since accumulation of CP24 is hampered when CP29 is missing, as previously reported [36]. Seedlings were grown for 5 weeks at 100 μmol photons m^{-2} s^{-1}, 23 °C, 70% humidity, and 8 h of daylight.

2.2. Membrane isolation

Dark-adapted leaves were rapidly homogenized using mortar and pestle, and stacked thylakoids were isolated as previously described [38], with the following modifications aimed at preserving thylakoid functionality: protease inhibitors (2 mM ε-aminocaproic acid, 2 mM benzamidine-hydrochloride, 0.5 mM PMSF) were added to the buffers; a maximum of 1 g of leaves was ground in 100 ml of GB; thylakoids were resuspended in B4 buffer (0.4 M sorbitol, 15 mM NaCl, 10 mM KCl, 5 mM $MgCl_2$, and 15 mM Hepes pH 7.8) before being frozen in liquid nitrogen.

2.3. Pigment analysis

Pigments were extracted from leaf disks with 85% acetone buffered with Na_2CO_3, then separated and quantified by HPLC [39].

2.4. In vivo fluorescence measurements

PSII maximal photochemical efficiency was measured through Chl fluorescence on dark-adapted leaves at room temperature with a PAM 101 fluorimeter (Walz, Germany); saturating light pulses (4500 μmol photons m^{-2} s^{-1}, 0.6 s) were supplied by a KL1500 halogen lamp (Schott, UK) (for results, please see Supplementary data).

2.5. Gel electrophoresis and immunoblotting

SDS-PAGE analysis was performed with the Tris–Tricine buffer system [40], with the addition of 7 M urea to the running gel when needed to separate Lhcb4 isoforms [36]. For fractionation of pigment–protein complexes, membranes corresponding to 500 μg of Chls were washed with 5 mM EDTA and then solubilized in 1 ml of 0.7% α-DM and 10 mM HEPES, pH 7.8. Solubilized samples were then fractionated by ultracentrifugation in a 0.1–1 M sucrose gradient containing 0.06% α-DM and 10 mM HEPES, pH 7.8 (22 h at 280,000 *g*, 4 °C). Non-denaturing Deriphat-PAGE was performed following the method developed in [41] with the modification described in [42]. The thylakoids concentrated at 1 mg/ml chlorophylls were solubilized with a final concentration of 1% α/β-DM, whereas 25 μg of Chls was loaded in each lane. Bands corresponding to trimeric LHCII and monomeric PSII core were excised from the gel, and purified complexes were then eluted by grinding gel slices in a buffer containing 10 mM Hepes pH 7.5 and 0.05% α-DM. LHCII/PSII core ratios were quantified by loading thylakoids (15 μg of Chls), PSII core (0.25–0.5–0.75–1.0 μg of Chls) and trimeric LHCII (1.0–2.0–3.0–4.0 μg of Chls) in the same slab gels. After staining with Coomassie blue, the signal amplitude of LHCII and CP43/CP47 bands were quantified ($n = 4$) by GelPro 3.2 software (Bio-Rad, USA). By using the pigment composition of the individual subunits [12,43] and the OD of each protein band, the number of LHCII trimers per monomeric PSII core was calculated. For immunotitration,

thylakoid samples corresponding to 0.1, 0.25, 0.5, and 1 μg of chlorophyll were loaded for each sample and electroblotted on nitrocellulose membranes; proteins were detected with alkaline phosphatase-conjugated antibody, according to Towbin et al. [44], and signal amplitude was quantified by densitometric analysis (n = 4). In order to avoid any deviation between different immunoblots, samples were compared only when loaded in the same slab gel.

2.6. Photosystem activity measured with artificial donors and acceptors

These measurements were performed as previously described [38]. PSI electron transport from the artificial donor ($TMPDH_2$, N,N,N,N-tetramethyl-p-phenylene-diamine, reduced form) to $NADP^+$ was measured at 22 °C on functional thylakoids in the dual-wavelength spectrophotometer Unicam AA (Thermo Scientific, USA), while PSII electron transport to DMBQ (dimethyl-benzoquinone) was measured following the O_2 evolution in a Clark-type oxygen electrode system (DW2/2, Hansatech Instruments, UK) both under red light illumination (200 μmol photons m^{-2} s^{-1}, λ > 600 nm). Concentrations used were as follows: 0.1 sorbitol, 5 mM $MgCl_2$, 10 mM NaCl, 20 mM KCl, 10 mM Hepes pH 7.8, 0.5 mM $NADP^+$, 10 μM Ferredoxin, either 300 mM DMBQ or 250 mM $TMPDH_2$ and thylakoids to a final Chl concentration of 10 μg/ml. When $TMPDH_2$ was used, the reaction mixture contained 5 mM ascorbic acid, and after 1.5 min of illumination 1 μM DCMU was added, followed by the artificial donor.

2.7. Time-resolved fluorescence

Time-correlated single photon counting (TCSPC) measurements were performed with a home-built setup [45,46]. In brief, samples were kept at room temperature (RT, 22 °C) in a flow cuvette coupled to a sample reservoir. The samples were flown from reservoir to cuvette with a speed of 2.5 ml/s and the optical path length of the cuvette was 3 mm. The samples were excited with 412 nm and 484 nm pulses of 0.2 ps duration at a repetition rate of 3.8 MHz. In order to avoid the closure of reaction centers the excitation intensity was kept low (0.5–1.5 μW) which resulted in a count rate of 30,000 photons per second or lower (see Supplementary data for details, Fig. S1). The diameter of the excitation spot was 2 mm. The instrument response function or IRF (70–80 ps FWHM) was obtained with pinacyanol iodide in methanol with a 6 ps fluorescence lifetime [47,48]. Measurements were done by collecting photons for 5 min. Fluorescence was detected at 679 nm, 701 nm and 720 nm using interference filters (15 nm width). The data were collected using a multichannel analyzer with a maximum time window of 4096 channels typically at 5 or 2 ps/channel. One complete experiment for a fluorescence decay measurement consisted of the recording of data sets of the reference compound, isolated thylakoid and again the reference compound, which was done at least three times in this order with a fresh sample for each condition, in order to check the reproducibility.

2.8. Data analysis

Data obtained with the TCSPC setup were globally analyzed using the "TRFA Data Processing Package" of the Scientific Software Technologies Center (Belarusian State University, Minsk, Belarus). Fluorescence decay curves were fitted to a sum of exponentials that was convoluted with the IRF. The quality of a fit was judged from the χ^2 value and by visual inspection of the residuals and the autocorrelation thereof. The number of exponentials was 5 in all cases, whereas one of these components was an artifact with a very fast lifetime (between 0.1 ps and 1 ps) which was mainly used to improve the fitting quality at early times. These artifacts are not further considered or discussed below.

3. Results

In order to isolate knock-out (KO) lines of *A. thaliana* lacking two or three minor antennae, kolhcb4.1, kolhcb4.2, kolhcb5 and kolhcb6 homozygous KO lines were identified in seed pools obtained from NASC by immunoblot analysis using specific antibodies raised against CP29, CP26 and CP24 antenna proteins, as previously described [36,37]. KO double mutants kolhcb5 kolhcb6 retain Lhcb4 (CP29) as the only minor antenna [37], while deletion of both CP29 isoforms in the kolhcb4.1 kolhcb4.2 double mutant results in a plant retaining CP26 as the only minor antenna, since accumulation of CP24 is hampered in this genotype [36]. Triple mutant kolhcb4.1 kolhcb4.2 kolhcb5 is lacking all minor antennae: indeed, deletion of both lhcb4.1 and lhcb4.2 yielded a plant devoid of CP29, and lack of CP29 hampered CP24 stability and accumulation [37]; thus the triple KO only retains subunits of the major antenna complex LHCII. In the following, we will refer to these genotypes as koCP26/24 (kolhcb5 kolhcb6), koCP29/24 (kolhcb4.1 kolhcb4.2) and NoM (kolhcb4.1 kolhcb4.2 kolhcb5). When grown in control conditions (100 μmol photons m^{-2} s^{-1}, 23 °C, 8/16 h day/night) for 4 weeks, koCP26/24 and koCP29/24 plants did not show significant reduction in growth with respect to the WT plants, while NoM plants were much smaller than WT plants (Fig. 1A). Thylakoid membranes were isolated from WT and mutant plants, and the lack of the corresponding gene product was confirmed by SDS-PAGE (Fig. 1B) and western blotting (see Supplementary data, Fig. S2). The pigment content of mutant thylakoids showed a significant decrease in the Chl *a*/Chl *b* ratio with respect to the membranes from WT (reflecting a relative increase of the amount of outer antenna

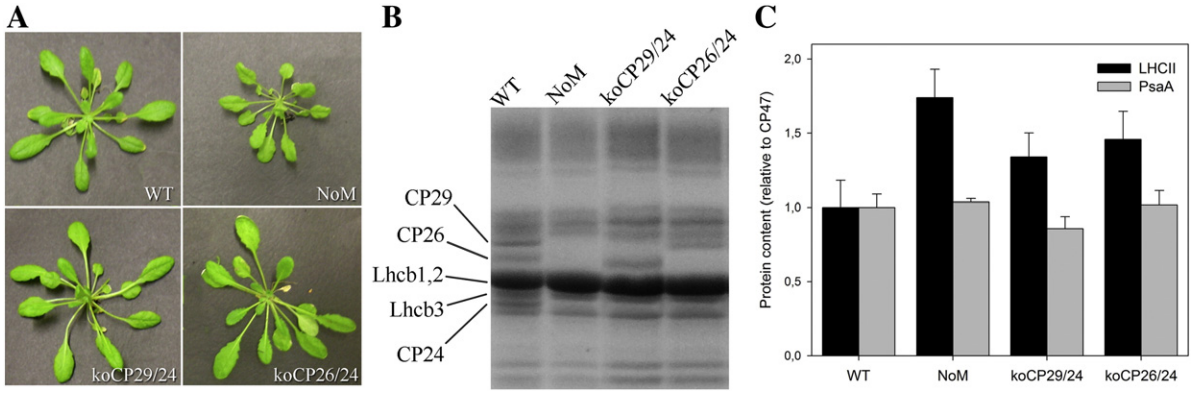

Fig. 1. Characterization of the KO mutants. (A) Phenotype of wild-type and mutant plants grown in control conditions (100 μmol photons m^{-2} s^{-1}, 23 °C, 8/16 h day/night) for 4 weeks. (B) SDS/PAGE analysis of wild-type and mutant thylakoid proteins. Selected apoprotein bands are marked. Fifteen micrograms of Chls were loaded in each lane. (C) Immunotitration of thylakoid proteins. Data of LHCII and PsaA subunits were normalized to the PSII core amount, CP47 content, and normalized to the corresponding WT content.

Table 1
Chlorophyll composition and LHCII content determined on thylakoids from wild-type and KO mutants.

Sample	Chl a/b	LHCII trimeric/PSII monomeric
WT	2.75 ± 0.05	4.2 ± 0.3
NoM	2.35 ± 0.04	6.1 ± 0.3
KoCP29/24	2.64 ± 0.03	4.8 ± 0.3
KoCP26/24	2.61 ± 0.02	5.1 ± 0.3

complexes): double mutants koCP26/24 and koCP29/24 showed a ratio of 2.61 and 2.64 respectively, *vs.* 2.75 for WT thylakoids. The lowest ratio (2.35) was observed for NoM (Table 1). In order to detect possible alterations in the relative amount of protein components of the photosynthetic apparatus upon removal of minor antennae, we determined the stoichiometry of the main subunits of both photosystems by immunoblotting titration, using antibodies specific for the subunits CP47 (PsbB, inner antenna of PSII core complex), PsaA (main subunit of PSI core complex) and LHCII (the major outer antenna of PSII). The PSI/PSII (PsaA/CP47) ratio was essentially the same in WT, koCP26/24 and NoM membranes, while a slight increase in CP47 relative content was detected for koCP29/24 as compared to WT. The LHCII/PSII ratio increased with the removing of monomeric antennae: both koCP26/24 and koCP29/24 had a significantly higher amount of LHCII with respect to WT, while the LHCII content was even higher in NoM (Fig. 1C). The stoichiometric ratio of trimeric LHCII and monomeric PSII core complex was determined by quantifying the Coomassie staining of the corresponding bands on an SDS/PAGE, by integrating the optical density of each band (see Supplementary data, Fig. S3; see Materials and methods for details). Results confirmed a far higher LHCII content in NoM (6.1 trimeric LHCII per monomeric PSII) with respect to the WT (4.2 trimers), while koCP29/24 and koCP26/24 showed an intermediate content (respectively, 4.8 and 5.1 trimers per monomeric PSII) (Table 1).

To analyze the organization of pigment–protein complexes, thylakoid membranes isolated from WT and KO mutants were solubilized with 0.7% dodecyl-α-D-maltoside (α-DM), then Chl-binding proteins were fractionated by sucrose gradient ultracentrifugation. The fractionation patterns are shown in Fig. 2. Six major green bands were obtained for the wild type: the PSI–LHCI complex was found as a major band in the lower part of the gradient, corresponding to a complex more stable than PSII that does not dissociate into smaller complexes upon mild solubilization of thylakoids; the PSII–LHCII components are visible as multiple green bands, namely PSII core complex, CP29–CP24–LHCII-M antenna supercomplex, trimeric LHCII and monomeric Lhcb; a large band with an apparent molecular mass higher than PSI–LHCI, which contained undissociated PSII supercomplexes of different LHCII compositions, was detected in the lower part of the gradient. The major difference detected in KO mutants with respect to the wild type was the lack of the antenna supercomplex CP29–CP24–LHCII. Moreover, PSII supercomplexes were differentially represented in these genotypes: faint bands of PSII supercomplexes were still detectable in the lower part of the gradient in both koCP29/24 and koCP26/24, although their amounts were strongly reduced as compared to WT, while NoM thylakoids were completely devoid of PSII supercomplexes.

To test the photosynthetic activity of both photosystems in our thylakoid preparations, artificial electron donors and acceptors were used. The rate of linear electron transport (ET) from H_2O to DMBQ, which accepts electrons at the Q_B site, was measured polarographically as the rate of O_2 evolution, while the ET capacity of PSI was measured spectrophotometrically as the rate of $NADP^+$ reduction, upon addition of the plastocyanin electron donor $TMPDH_2$ (see Materials and methods for details). Results reported in Table S1 show that all photosystems retained their ET capacity, which clearly indicates that all the preparations are active and can efficiently drive photosynthesis. However, a reduction in O_2 evolution and NADPH accumulation on a Chl basis was observed in the membranes of NoM mutants (respectively, −30% and −20% as compared with the WT); this result might be ascribed to a lower PSII efficiency due to the presence of badly connected LHCII in the NoM mutant as compared to WT.

Fluorescence decay curves were measured with the TCSPC setup stacked thylakoids from *A. thaliana*. This approach aimed to be close to the native situation and was preferred above measuring on grana-enriched membranes (BBYs), which are known to constitute a heterogeneous system and to retain a far lower amount of trimeric LHCII than the number generally reported to be bound per RC in thylakoid preparations. Either 412-nm laser pulses, exciting relatively more PSII core complexes, or 484 nm laser pulses, exciting relatively more outer antenna complexes, were used. For detection 679 nm-, 701 nm- and 720 nm-interference band filters were used. By combining the results for different excitation and detection wavelengths it is in principle possible to differentiate between PSI and PSII kinetics and to estimate the average migration time of excitations to the PSII reaction centers [25].

The fluorescence decay curves of thylakoid preparations from WT, NoM, koCP29/24 and koCP26/24 mutants were strikingly different from each other (Fig. 3). The decay of WT thylakoids was the fastest

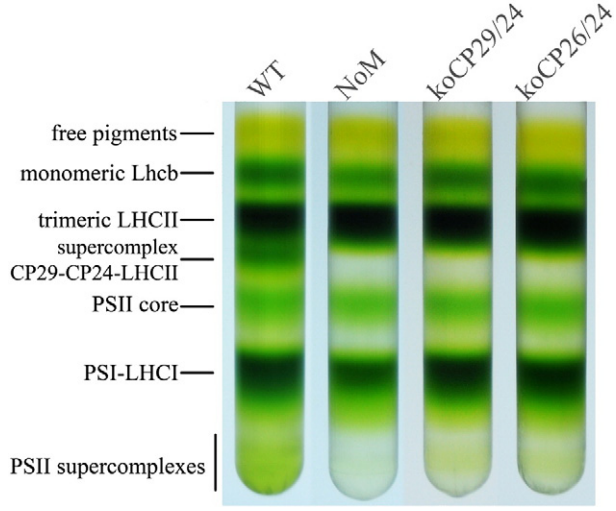

Fig. 2. Sucrose density gradient fractionation of wild-type and KO mutant solubilized thylakoids. Solubilization was performed with 0.7% α-DM. Composition of the green bands are indicated.

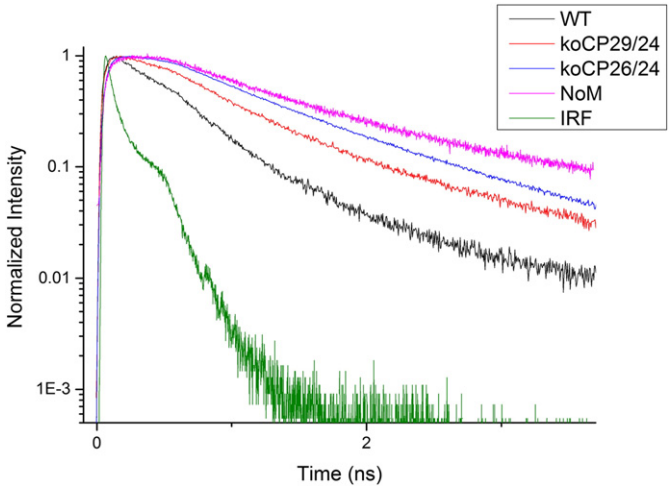

Fig. 3. Time-resolved fluorescence decays of thylakoid membranes from WT, KoCP29/24, KoCP26/24 and NoM strains. The excitation wavelength is 412 nm and the detection wavelength is 680 nm.

Table 2
Fitted lifetimes (and amplitudes in brackets) for thylakoids at room temperature with an excitation wavelength of 412 nm and a detection wavelength of 680 nm.

	WT	koCP2624	koCP29CP24	NoM
τ_1	52 ps (25%)	64 ps (23%)	66 ps (21%)	59 ps (30%)
τ_2	166 ps (32%)	273 ps (23%)	278 ps (23%)	294 ps (20%)
τ_3	409 ps (42%)	912 ps (53%)	732 ps (52%)	1.001 ns (48%)
τ_4	5.6 ns (1%)	2.8 ns (1%)	2.1 ns (4%)	2.9 ns (2%)

Confidence intervals of fluorescence lifetimes (τ) as calculated by exhaustive search were <5%; lifetimes were calculated from 2 to 6 repeats.

followed by those of koCP29/24, koCP26/24 and NoM, in that order. To get more quantitative information from the decay curves, they were fitted to a sum of exponential decay functions. The fitting results are given in Table 2 (more detailed results are given in Supplementary data, see Table S2, Table S3, Table S4 and Table S5).

The lifetime τ_1, which is in the range of 50 ps–70 ps, is largely due to PSI, although also PSII does contribute to some extent [25,28,49]. Because PSI fluorescence is red-shifted as compared to PSII fluorescence, the relative amplitude of this component increases upon going from detection wavelength 679 to 720 nm. The value of τ_1 and the corresponding amplitude only differ to a limited extent for the different thylakoid preparations. WT *Arabidopsis* shows the shortest value for τ_1 with 52 ps, whereas the τ_1 value for the NoM mutant is only 7 ps slower (59 ps). The τ_1 value is somewhat slower for koCP26/24 and koCP29/24 with 64 ps and 66 ps, respectively. The relative amplitude of τ_1 ranges from 21 to 30% for the different thylakoid preparations (for $\lambda_{exc} = 412$ nm, $\lambda_{det} = 679$ nm; more detailed results are given in Supplementary data; see Table S2, Table S3, Table S4 and Table S5).

The lifetimes τ_2 and τ_3 in Table 2 are mainly due to PSII–LHCII (and possibly some detached antenna with the highest amplitude at $\lambda_{det} = 679$ nm, as expected for PSII–LHCII) [25]. WT thylakoids show the lowest values for both τ_2 (166 ps) and τ_3 (409 ps). These lifetimes become considerably longer for the mutants. The τ_2 values for the various mutants are very similar to each other, ranging from 273 ps to 294 ps. On the other hand, the difference in τ_3 for the mutants is significantly more pronounced. τ_3 is 732 ps for the koCP29/24 mutant, whereas it is 905 ps for koCP26/24 and 1.00 ns for NoM. In comparison to WT, the amplitude for τ_3 becomes rather high in all mutants whereas the amplitudes for τ_2 decrease substantially. Finally, the slowest component (τ_4) can be ascribed to free chlorophyll and/or disconnected light-harvesting complexes with very low amplitudes and possibly some closed RCs although this is rather unlikely with the current excitation conditions (total amplitude is at most 4%) [25]. It should be noted that the amplitude for τ_4 is lower than 1% for WT thylakoids (detailed results are given in Supplementary data, see Table S2, Table S3, Table S4 and Table S5).

To estimate the PSII–LHCII kinetics, PSI and PSII kinetics were separated from each other using the method recently presented by van Oort et al. [25]. In brief, the PSII–LHCII contribution to the sub-100 ps component was determined by using different excitation and detection wavelengths [25] and together with the long lifetimes τ_2 and τ_3, which are solely attributed to PSII–LHCII, the kinetics of PSII–LHCII, with possibly some free LHCII, can be calculated [25]. The obtained PSII–LHCII kinetics differ considerably for WT and mutant thylakoids. For excitation at 412 nm, the WT preparation shows the fastest PSII–LHCII kinetics with an average lifetime of 259 ps, whereas the mutants are significantly slower; 523 for koCP29/24, 617 ps for koCP26/24, and 601 ps for NoM. For excitation at 484 nm, the PSII–LHCII kinetics of all mutant and WT preparations become slower. The PSII–LHCII average lifetime for WT cells is then 285 ps. For the mutant preparations, the average lifetimes are 565 ps, 687 ps and 771 ps for koCP29/24, koCP26/24 and NoM, respectively (Table 3).

The difference in PSII–LHCII average lifetime for different excitation wavelengths is approximately proportional to the average migration time of excitons needed to reach the RC for the first time, but the presence of detached antennae also affects this difference. The difference is 26 ps for WT thylakoids, whereas it becomes larger for the mutants: 41 ps and 70 ps for koCP29/24 and koCP26/24, respectively, whereas it is even 170 ps for NoM mutants. It should be noted that detached or loosely bound antennae cause a significant increase of the difference between PSII–LHCII kinetics for different excitation wavelengths (Table 3). In addition, it should be mentioned that the difference between overall average lifetimes (*i.e.* without correction for PSI) with different excitation wavelengths for WT and mutant strains has the same trend as the difference in PSII–LHCII average lifetime for different excitation wavelengths (see Supplementary data Table S2, Table S3, Table S4 and Table S5), which shows that the differences between corrected lifetimes upon different excitation wavelengths are not artificially created or exaggerated because of corrections and calculations. The calculated PSII–LHCII average lifetime values will be discussed hereafter.

Table 3
PSII–LHCII (with possible free LHCII) kinetics for thylakoid membranes.

Excitation	τ_{avg} (ps)		Difference (ps)
	412 nm	484 nm	
WT	259	285	26
KoCP29/24	523	565	42
KoCP26/24	617	687	70
NoM	601	778	178

The PSII–LHCII (with possible free LHCII) kinetics were derived from the kinetics of thylakoid membranes by removing the PSI contribution, as explained in van Oort et al. [25] before.

4. Discussion

The monomeric antennae CP24, CP26, and CP29 are three of the six light-harvesting subunits that compose the PSII peripheral antenna system of higher plants. They are the only Lhc subunits that can occupy the position between the inner antennae CP43/CP47 and the outer LHCII trimers within the PSII supercomplex [50] (Fig. 4). Although these pigment–protein complexes are homologous and are expected to share a common three-dimensional organization on the basis of the structural data available [43,51], they cannot be exchanged between each other in the supercomplexes [50].

Earlier work [52] has characterized *Arabidopsis* plants devoid of LHCII, and proposed a high degree of redundancy among Lhcb subunits; indeed, the PSII supercomplex organization was maintained in the absence of LHCII by over-accumulating Lhcb5. Instead, the knock-out of monomeric antennae leads to destabilization of PSII–Lhcb supercomplexes, meaning that the minor antennae are essential for PSII organization. This conclusion is supported by the fact that removal of two or more different monomeric Lhcbs increases the trapping time of excitons in the RCs substantially as compared to WT thylakoids, meaning that the absence of minor antenna complexes leads to badly connected or disconnected LHCII as will be discussed further below.

Recently, time-resolved fluorescence kinetic studies were performed on different knockout mutants of *A. thaliana*. It was shown that, in the absence of specific minor antenna complexes in most cases the overall average lifetimes become longer as compared to those of WT cells [25,30] and in particular the migration time of excitations to the RCs increases [25,30]. These results confirm that there are disruptions of the PSII–LHCII complex organization in the absence of minor antenna complexes resulting in the formation of badly connected or disconnected LHCII [25,30]. Among the mutants studied here, the most explicit slowdown of the fluorescence kinetics is observed for the NoM mutant as might have been expected since all minor antenna complexes are missing. For koCP26/24 the slowdown of the fluorescence kinetics is more pronounced than for koCP29/24. This observation is in good agreement with previous work in [30], which indicates that both double mutants have disconnected LHCII, but the koCP26/24

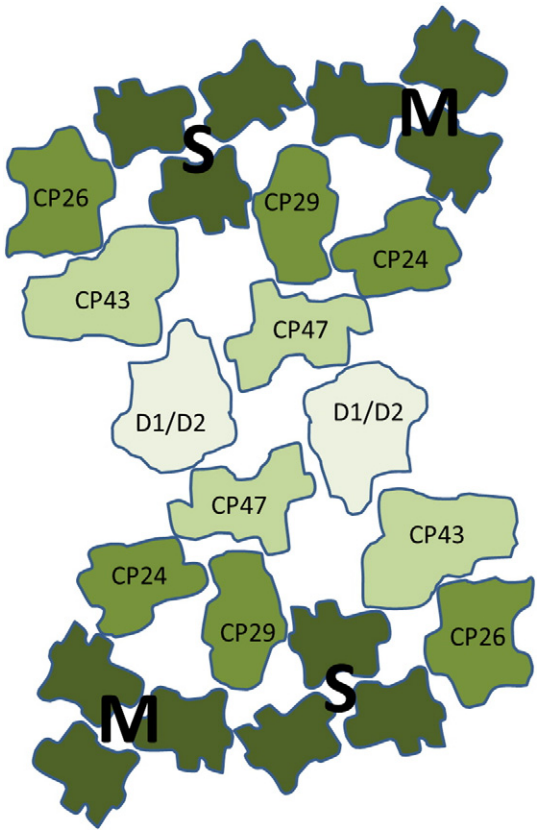

Fig. 4. Membrane organization of PSII in *Arabidopsis thaliana*. The core of PSII consists of the reaction center (D1/D2) together with CP47 and CP43. Minor antenna complexes (CP24, CP26 and CP29) with the major antenna complexes LHCII (dark green) form peripheral antenna that surrounds the core. The binding strength of trimeric LHCII at different locations is strong (S) or moderate (M). PSII structure is based on the study of Caffari et al. [22].

mutant has more, although the mutant that was lacking CP26 showed faster fluorescence kinetics than mutants lacking either CP24 or CP29 or both [25].

The most significant increase concerns the lifetimes of decay components 2 and 3 for all mutants, and this must originate from a reorganization or "disassembly" of PSII–LHCII, in agreement with earlier studies [25,30]. The increase in the lifetime of the PSII–LHCII components can be explained by the existence of badly connected or disconnected LHCII due to the absence of several minor antenna complexes. In the presence of disconnected LHCII, long-lived fluorescence components (around 4 ns) are expected, unless the LHCII complexes aggregate [48] which leads to a shortening of the fluorescence lifetime [48]. In a previous picosecond fluorescence study on thylakoid membranes from *A. thaliana*, it was shown that not only lifetime components 2 and 3 are responsible for the PSII–LHCII kinetics, but component 1 is also partly due to PSII–LHCII [25]. In that study, van Oort et al. used two excitation wavelengths in order to vary the relative amount of excitations in the core and outer antenna of PSII [25]. Applying this method, we find that the average lifetime of PSII–LHCII for the NoM mutant is 2.3 times longer than the average lifetime of PSII–LHCII for WT. This huge difference is attributed to the disruption of PSII supercomplexes and the presence of detached LHCII. Furthermore, from the biochemical analysis it is concluded that the LHCII/PSII ratio is increased by 50% in the NoM mutant as compared to WT cells, which means that the number of PSII pigments per RC in the NoM mutant is about 20% higher than in WT, since monomeric antennae are lacking. This should lead to an increase of the average lifetime of approximately 20% if all LHCII would be connected equally well to the PSII RC as in WT thylakoids [25]. To figure out the reason behind the increase of the average lifetime, the migration time for the WT and NoM mutant are calculated by the method van Oort et al. [25]. According to this method, the difference $\Delta\tau$ in the average lifetime of PSII for the two excitation wavelengths is approximately proportional to the migration time [25]. For WT cells we find $\Delta\tau = 26$ ps, whereas for the NoM mutant the value of $\Delta\tau$ is far larger, *i.e.* 170 ps. This dramatic increase cannot be explained by an increase of the migration time because of badly connected LHCII only but there should also be a significant fraction of disconnected LHCII (see also Van Oort et al. 2010). The (partial) detachment of LHCII is confirmed by the absence in NoM mutants of PSII supercomplexes containing LHCII-S, as shown upon mild solubilization of thylakoids and fractionation of pigment–protein complexes by ultracentrifugation (Fig. 2). Therefore, CP29 and CP26 play a crucial role in mediating the association of trimeric LHCII with the PSII complex. Moreover, the loss of all monomeric Lhcbs was accompanied by an over-accumulation of LHCII (+45% as compared to WT), suggesting compensation within the group of Lhcb proteins as a general regulatory mechanism for PSII antenna size. The phenotype of NoM is consistent with a recent study of *A. thaliana* acclimation to low- *vs.* high-light [53], which showed that LHCII is, among the Lhcbs, the major one responsible for the regulation of the PSII antenna size during acclimation.

The efficiency of light harvesting, directly related to the plastoquinone redox state, might play a role in antenna-size regulation. Indeed, the redox state is an indicator of the overall efficiency of photosynthetic electron transport, and it was suggested to play a key role in the modulation of antenna size through regulation of the Lhc genes expression [54]. More recent results [55] showed than upon long-term acclimation, despite a lack of Lhcb transcriptional regulation, the level of LHCII is tuned to environmental conditions, thus suggesting that the steady-state level of LHCII depends on post-transcriptional, rather than on transcriptional regulation, as assessed by the finding of a strong differential translational control on individual Lhcb mRNAs [56]. Thus, overaccumulation of LHCII in NoM would represent an adaptation response: depletion of minor antennae leads to reduced trapping efficiency in limiting light, and would trigger a compensative response leading to a photosynthetic phenotype with high LHCII/PSII ratio, namely resembling that of low light-acclimated leaves.

Accumulation of a large amount of disconnected antenna proteins in the NoM thylakoids suggests that LHCII is independently folded into membranes, irrespective from its assembly with the PSII core complex later on [57]. Therefore, even when assembly is prevented, LHCII is stable in the membrane and does not undergo proteolytic degradation. This evidence is consistent with the phenotype of PSII mutants such as *viridis-zd*^{69} of barley [58] and of lincomycin-treated plants [59], which revealed the stability of free LHCII in the thylakoids.

Isolation of the C_2S_2 supercomplex from koCP29/24 thylakoid membranes [36] has shown that LHCII-S can be associated with the core complex when CP26 is the only monomeric subunit present. This evidence is consistent with the isolation of a stable monomeric core with CP26 and the LHCII-S trimer [20]. In the absence of both CP29 and CP24, some $C_2S_2M_2$ complexes can assemble in grana membranes, but they are less stable and the molecular interactions are rather weak [36]. Moreover, koCP29/24 plants show a 15% increase in LHCII content with respect to the wild-type level (similar to the 20% for the koCP26/24 mutant). Thus, it is likely that a large part of the outer antenna is not directly bound to the PSII supercomplexes; rather, other trimers are interspersed among the C_2S_2 particles. This is confirmed by the time-resolved fluorescence data. The PSII–LHCII kinetics slows down significantly (average lifetime is almost doubled as compared to WT) while the value of $\Delta\tau$ is 42 ps as compared to 26 ps for WT. In a previous study, a CP29 antisense line was studied with the same method that we used here and the results are slightly different [25]. In that case $\Delta\tau$ was 30 ps instead of 42 ps [25]. However, it should be mentioned that in the CP29 antisense mutant CP29 expression was only partially blocked [60] as shown by detection of CP24 unlike the present mutant [36]. For koCP29/24 a large fraction of uncoupled LHCII is observed,

giving rise to a long lifetime of 732 ps (see τ_3 in Tables 2 and S3). In addition, after correcting for the PSI contribution and the 2 ns component the corresponding amplitude is around 65%, depending somewhat on excitation wavelength. For koCP26/24 the fitted lifetime is 912 ps with a similar amplitude around 64% after correcting for the PSI contribution. These amplitudes might correspond to the percentage of badly connected Chls *a* and since there are 5 LHCII trimers per PSII core in each mutant, this implies that at most one LHCII trimer plus one minor antenna, either CP29 or CP26 depending on the type of mutant, would be closely associated with the PSII core. This is in excellent agreement with earlier work in which it was shown that LHCII-S can be associated with the core complex when CP26 is the only monomeric subunit present [36]. Such an interpretation of the lifetime data would be in agreement with electron-microscopy observations, which show a high number of LHCII complexes interposed between rows of connected PSII cores in grana membranes [37]. These results would also be consistent with recent biochemical characterization of PSII supercomplexes in *Arabidopsis* [20], which indicates that LHCII-S binding is far less stable in a mutant devoid of CP26. The absence of a PSII supercomplex binding LHCII-M indicates that CP26 and CP24 have an important function in mediating the association of the $C_2S_2M_2$ complex.

A key consideration for the efficiency of primary productivity in plants and algae is the size of the light-harvesting system. Ort, Zhu and Melis have proposed antenna size reduction as a valuable strategy for the optimisation of the light reactions: theoretical simulation of net CO_2 uptake suggested that a smaller antenna size would significantly improve photosynthetic efficiency on crop canopies [61]. Even biomass yield of microalgal cultures at industrial scale is currently limited by several biological constraints, including the uneven light distribution into photobioreactors [62]; therefore, the successful implementation of biofuel production facilities requires domestication strategies, such as decreasing the absorption cross section to enhance light penetration and increase the size of metabolic sinks per chlorophyll [63,64].

However, strategies to improve light penetration must ensure that truncated antenna mutants are not photosynthetically impaired in ways other than reduced LHC content: indeed in higher plants, an extreme reduction in LHC complement leads to a lower photochemical yield and increases photoinhibition [65].

The present results show that depletion of even a sub-group of LHCs strongly affects the PSII light-harvesting efficiency and thus the photoautotrophic growth. To ensure that truncated-antenna strains will operate with improved light use efficiency, biotechnological approaches aimed at reducing antenna cross-section must focus on trimeric LHCII, rather than monomeric Lhcb, content: the latter leads to a strong impairment of PSII light-use efficiency, thus canceling out benefits of optical density reduction, although only for the NoM mutant this leads to strongly reduced growth under continuous-light conditions.

In summary, we have found in this study that in the absence of all minor antenna complexes of PSII, the functional connection of LHCII to the PSII cores is strongly diminished. A large part of this LHCII has a long excited-state lifetime although far shorter than the 4 ns of isolated LHCII trimers. Most likely, the detached LHCII is aggregated which leads to a shortening of the excited-state lifetime. In koCP26/24 and koCP29/24 mutants, it seems likely that only one LHCII trimer is directly (specifically) connected to the PSII core (or two LHCII trimers per PSII core dimer) whereas all other trimers are interspersed between the supercomplexes and still lead to relatively good EET, not hampering plant growth during continuous growth light conditions.

Acknowledgements

We thank Roberto Bassi for helpful discussions and support. This work was supported financially by the Netherlands Organization for Scientific Research (NWO) *via* the Council for Chemical Sciences (HvA) (Project number: 700.59.016).

Appendix A. Supplementary data

Supplementary data to this article can be found online at http://dx.doi.org/10.1016/j.bbabio.2014.09.011.

References

[1] N. Nelson, A. Ben-Shem, The complex architecture of oxygenic photosynthesis, Nat. Rev. Mol. Cell Biol. 5 (2004) 971–982.
[2] R. Croce, H. van Amerongen, Natural strategies for photosynthetic light harvesting, Nat. Chem. Biol. 10 (2014) 492–501.
[3] N. Nelson, C.F. Yocum, Structure and function of photosystems I and II, Annu. Rev. Plant Biol. 57 (2006) 521–565.
[4] J. Veerman, F.K. Bentley, J.J. Eaton-Rye, C.W. Mullineaux, S. Vasil'ev, D. Bruce, The PsbU subunit of photosystem II stabilizes energy transfer and primary photochemistry in the phycobilisome — photosystem II assembly of *Synechocystis* sp. PCC 6803, Biochemistry 44 (2005) 16939–16948.
[5] H. van Amerongen, R. Croce, Light harvesting in photosystem II, Photosynth. Res. 116 (2013) 251–263.
[6] G.H. Schatz, H. Brock, A.R. Holzwarth, Kinetic and energetic model for the primary processes in photosystem-II, Biophys. J. 54 (1988) 397–405.
[7] R. Croce, H. van Amerongen, Light-harvesting in photosystem I, Photosynth. Res. 116 (2013) 153–166.
[8] A. Busch, M. Hippler, The structure and function of eukaryotic photosystem I, Biochim. Biophys. Acta Bioenerg. 1807 (2011) 864–877.
[9] A.N. Melkozernov, S. Lin, R.E. Blankenship, Excitation dynamics and heterogeneity of energy equilibration in the core antenna of photosystem I from the cyanobacterium *Synechocystis* sp. PCC 6803, Biochemistry 39 (2000) 1489–1498.
[10] B. Gobets, R. van Grondelle, Energy transfer and trapping in photosystem I, Biochim. Biophys. Acta Bioenerg. 1507 (2001) 80–99.
[11] K.N. Ferreira, T.M. Iverson, K. Maghlaoui, J. Barber, S. Iwata, Architecture of the photosynthetic oxygen-evolving center, Science 303 (2004) 1831–1838.
[12] Y. Umena, K. Kawakami, J.R. Shen, N. Kamiya, Crystal structure of oxygen-evolving photosystem II at a resolution of 1.9 Angstrom, Nature 473 (2011) 55–60.
[13] E.J. Boekema, H. van Roon, J.F.L. van Breemen, J.P. Dekker, Supramolecular organization of photosystem II and its light-harvesting antenna in partially solubilized photosystem II membranes, Eur. J. Biochem. 266 (1999) 444–452.
[14] S.S. Lampoura, V. Barzda, G.M. Owen, A.J. Hoff, H. van Amerongen, Aggregation of LHCII leads to a redistribution of the triplets over the central xanthophylls in LHCII, Biochemistry 41 (2002) 9139–9144.
[15] M. Mozzo, L. Dall'Osto, R. Hienerwadel, R. Bassi, R. Croce, Photoprotection in the antenna complexes of photosystem II — role of individual xanthophylls in chlorophyll triplet quenching, J. Biol. Chem. 283 (2008) 6184–6192.
[16] V. Barzda, E.J.G. Peterman, R. van Grondelle, H. van Amerongen, The influence of aggregation on triplet formation in light-harvesting chlorophyll a/b pigment–protein complex II of green plants, Biochemistry 37 (1998) 546–551.
[17] N. Betterle, M. Ballottari, S. Zorzan, S. de Bianchi, S. Cazzaniga, L. Dall'Osto, T. Morosinotto, R. Bassi, Light-induced dissociation of an antenna hetero-oligomer is needed for non-photochemical quenching induction, J. Biol. Chem. 284 (2009) 15255–15266.
[18] P. Horton, A.V. Ruban, R.G. Walters, Regulation of light harvesting in green plants, Annu. Rev. Plant Physiol. Plant Mol. Biol. 47 (1996) 655–684.
[19] E.C.M. Engelmann, G. Zucchelli, F.M. Garlaschi, A.P. Casazza, R.C. Jennings, The effect of outer antenna complexes on the photochemical trapping rate in barley thylakoid photosystem II, Biochim. Biophys. Acta Bioenerg. 1706 (2005) 276–286.
[20] S. Caffarri, R. Kouril, S. Kereiche, E.J. Boekema, R. Croce, Functional architecture of higher plant photosystem II supercomplexes, EMBO J. 28 (2009) 3052–3063.
[21] S. Caffarri, K. Broess, R. Croce, H. van Amerongen, Excitation energy transfer and trapping in higher plant photosystem II complexes with different antenna sizes, Biophys. J. 100 (2011) 2094–2103.
[22] S. de Bianchi, M. Ballottari, L. Dall'Osto, R. Bassi, Regulation of plant light harvesting by thermal dissipation of excess energy, Biochem. Soc. Trans. 38 (2010) 651–660.
[23] D.G. Durnford, J.A. Price, S.M. McKim, M.L. Sarchfield, Light-harvesting complex gene expression is controlled by both transcriptional and post-transcriptional mechanisms during photoacclimation in *Chlamydomonas reinhardtii*, Physiol. Plant. 118 (2003) 193–205.
[24] K. Broess, G. Trinkunas, A. van Hoek, R. Croce, H. van Amerongen, Determination of the excitation migration time in photosystem II — consequences for the membrane organization and charge separation parameters, Biochim. Biophys. Acta Bioenerg. 1777 (2008) 404–409.
[25] B. van Oort, M. Alberts, S. de Bianchi, L. Dall'Osto, R. Bassi, G. Trinkunas, R. Croce, H. van Amerongen, Effect of antenna-depletion in photosystem II on excitation energy transfer in *Arabidopsis thaliana*, Biophys. J. 98 (2010) 922–931.
[26] G.H. Schatz, H. Brock, A.R. Holzwarth, Picosecond kinetics of fluorescence and absorbance changes in photosystem II particles excited at low photon density, Proc. Natl. Acad. Sci. U. S. A. 84 (1987) 8414–8418.
[27] R. Vangrondelle, Excitation-energy transfer, trapping and annihilation in photosynthetic systems, Biochim. Biophys. Acta 811 (1985) 147–195.
[28] E. Wientjes, H. van Amerongen, R. Croce, LHCII is an antenna of both photosystems after long-term acclimation, Biochim. Biophys. Acta 1827 (2013) 420–426.
[29] E. Wientjes, H. van Amerongen, R. Croce, Quantum yield of charge separation in photosystem II: functional effect of changes in the antenna size upon light acclimation, J. Phys. Chem. B 117 (2013) 11200–11208.

[30] Y. Miloslavina, S. de Bianchi, L. Dall'Osto, R. Bassi, A.R. Holzwarth, Quenching in *Arabidopsis thaliana* mutants lacking monomeric antenna proteins of photosystem II, J. Biol. Chem. 286 (2011) 36830–36840.
[31] D.I.G. Bennett, K. Amarnath, G.R. Fleming, A structure-based model of energy transfer reveals the principles of light harvesting in photosystem II supercomplexes, J. Am. Chem. Soc. 135 (2013) 9164–9173.
[32] J. Chmeliov, G. Trinkunas, H. van Amerongen, L. Valkunas, Light harvesting in a fluctuating antenna, J. Am. Chem. Soc. 136 (2014) 8963–8972.
[33] J.P. Dekker, R. Van Grondelle, Primary charge separation in photosystem II, Photosynth. Res. 63 (2000) 195–208.
[34] V.I. Novoderezhkin, E.G. Andrizhiyevskaya, J.P. Dekker, R. van Grondelle, Pathways and timescales of primary charge separation in the photosystem II reaction center as revealed by a simultaneous fit of time-resolved fluorescence and transient absorption, Biophys. J. 89 (2005) 1464–1481.
[35] M.K. Sener, C. Jolley, A. Ben-Shem, P. Fromme, N. Nelson, R. Croce, K. Schulten, Comparison of the light-harvesting networks of plant and cyanobacterial photosystem I, Biophys. J. 89 (2005) 1630–1642.
[36] S. de Bianchi, N. Betterle, R. Kouril, S. Cazzaniga, E. Boekema, R. Bassi, L. Dall'Osto, *Arabidopsis* mutants deleted in the light-harvesting protein Lhcb4 have a disrupted photosystem II macrostructure and are defective in photoprotection, Plant Cell 23 (2011) 2659–2679.
[37] S. de Bianchi, L. Dall'Osto, G. Tognon, T. Morosinotto, R. Bassi, Minor antenna proteins CP24 and CP26 affect the interactions between photosystem II subunits and the electron transport rate in grana membranes of *Arabidopsis*, Plant Cell 20 (2008) 1012–1028.
[38] A.P. Casazza, D. Tarantino, C. Soave, Preparation and functional characterization of thylakoids from *Arabidopsis thaliana*, Photosynth. Res. 68 (2001) 175–180.
[39] A.M. Gilmore, H.Y. Yamamoto, Zeaxanthin formation and energy-dependent fluorescence quenching in pea-chloroplasts under artificially mediated linear and cyclic electron-transport, Plant Physiol. 96 (1991) 635–643.
[40] H. Schagger, G. Vonjagow, Tricine sodium dodecyl-sulfate polyacrylamide-gel electrophoresis for the separation of proteins in the range from 1-kDa to 100-kDa, Anal. Biochem. 166 (1987) 368–379.
[41] G.F. Peter, J.P. Thornber, Biochemical-composition and organization of higher-plant photosystem-II light-harvesting pigment-proteins, J. Biol. Chem. 266 (1991) 16745–16754.
[42] M. Havaux, L. Dall'Osto, S. Cuine, G. Giuliano, R. Bassi, The effect of zeaxanthin as the only xanthophyll on the structure and function of the photosynthetic apparatus in *Arabidopsis thaliana*, J. Biol. Chem. 279 (2004) 13878–13888.
[43] Z.F. Liu, H.C. Yan, K.B. Wang, T.Y. Kuang, J.P. Zhang, L.L. Gui, X.M. An, W.R. Chang, Crystal structure of spinach major light-harvesting complex at 2.72 Angstrom resolution, Nature 428 (2004) 287–292.
[44] H. Towbin, T. Staehelin, J. Gordon, Electrophoretic transfer of proteins from polyacrylamide gels to nitrocellulose sheets — procedure and some applications, Proc. Natl. Acad. Sci. U. S. A. 76 (1979) 4350–4354.
[45] O.J.G. Somsen, L.B. Keukens, M.N. de Keijzer, A. van Hoek, H. van Amerongen, Structural heterogeneity in DNA: temperature dependence of 2-aminopurine fluorescence in dinucleotides, ChemPhysChem 6 (2005) 1622–1627.
[46] J.W. Borst, M.A. Hink, A. van Hoek, A.J.W.G. Visser, Effects of refractive index and viscosity on fluorescence and anisotropy decays of enhanced cyan and yellow fluorescent proteins, J. Fluoresc. 15 (2005) 153–160.
[47] B. van Oort, A. Amunts, J.W. Borst, A. van Hoek, N. Nelson, H. van Amerongen, R. Croce, Picosecond fluorescence of intact and dissolved PSI–LHCI crystals, Biophys. J. 95 (2008) 5851–5861.
[48] B. van Oort, A. van Hoek, A.V. Ruban, H. van Amerongen, Aggregation of Light-Harvesting Complex II leads to formation of efficient excitation energy traps in monomeric and trimeric complexes, FEBS Lett. 581 (2007) 3528–3532.
[49] R. Croce, H. van Amerongen, Light-harvesting and structural organization of photosystem II: from individual complexes to thylakoid membrane, J. Photochem. Photobiol. B Biol. 104 (2011) 142–153.
[50] H. van Amerongen, J.P. Dekker, Light harvesting in photosystem II, Light-harvesting antennas in photosynthesis, Kluwer Academic Publishers, 2003, pp. 219–251.
[51] X.W. Pan, M. Li, T. Wan, L.F. Wang, C.J. Jia, Z.Q. Hou, X.L. Zhao, J.P. Zhang, W.R. Chang, Structural insights into energy regulation of light-harvesting complex CP29 from spinach, Nat. Struct. Mol. Biol. 18 (2011) 309–315.
[52] A.V. Ruban, M. Wentworth, A.E. Yakushevska, J. Andersson, P.J. Lee, W. Keegstra, J.P. Dekker, E.J. Boekema, S. Jansson, P. Horton, Plants lacking the main light-harvesting complex retain photosystem II macro-organization, Nature 421 (2003) 648–652.
[53] M. Ballottari, L. Dall'Osto, T. Morosinotto, R. Bassi, Contrasting behavior of higher plant photosystem I and II antenna systems during acclimation, J. Biol. Chem. 282 (2007) 8947–8958.
[54] J.M. Escoubas, M. Lomas, J. Laroche, P.G. Falkowski, Light-intensity regulation of cab gene-transcription is signaled by the redox state of the plastoquinone pool, Proc. Natl. Acad. Sci. U. S. A. 92 (1995) 10237–10241.
[55] S. Frigerio, C. Campoli, S. Zorzan, L.I. Fantoni, C. Crosatti, F. Drepper, W. Haehnel, L. Cattivelli, T. Morosinotto, R. Bassi, Photosynthetic antenna size in higher plants is controlled by the plastoquinone redox state at the post-transcriptional rather than transcriptional level, J. Biol. Chem. 282 (2007) 29457–29469.
[56] M. Floris, R. Bassi, C. Robaglia, A. Alboresi, E. Lanet, Post-transcriptional control of light-harvesting genes expression under light stress, Plant Mol. Biol. 82 (2013) 147–154.
[57] N.H. Chua, P. Bennoun, Thylakoid membrane polypeptides of *Chlamydomonas reinhardtii* — wild-type and mutant strains deficient in photosystem 2 reaction center, Proc. Natl. Acad. Sci. U. S. A. 72 (1975) 2175–2179.
[58] O. Machold, D.J. Simpson, B.L. Moller, Chlorophyll-proteins of thylakoids from wild-type and mutants of barley (*Hordeum vulgare* L.), Carlsb. Res. Commun. 44 (1979) 235–254.
[59] L. Gaspar, E. Sarvari, F. Morales, Z. Szigeti, Presence of 'PSI free' LHCI and monomeric LHCII and subsequent effects on fluorescence characteristics in lincomycin treated maize, Planta 223 (2006) 1047–1057.
[60] J. Andersson, R.G. Walters, P. Horton, S. Jansson, Antisense inhibition of the photosynthetic antenna proteins CP29 and CP26: implications for the mechanism of protective energy dissipation, Plant Cell 13 (2001) 1193–1204.
[61] D.R. Ort, X.G. Zhu, A. Melis, Optimizing antenna size to maximize photosynthetic efficiency, Plant Physiol. 155 (2011) 79–85.
[62] P.G. Stephenson, C.M. Moore, M.J. Terry, M.V. Zubkov, T.S. Bibby, Improving photosynthesis for algal biofuels: toward a green revolution, Trends Biotechnol. 29 (2011) 615–623.
[63] J.E.W. Polle, S.D. Kanakagiri, A. Melis, tla1, a DNA insertional transformant of the green alga *Chlamydomonas reinhardtii* with a truncated light-harvesting chlorophyll antenna size, Planta 217 (2003) 49–59.
[64] H. Kirst, J.G. Garcia-Cerdan, A. Zurbriggen, T. Ruehle, A. Melis, Truncated photosystem chlorophyll antenna size in the green microalga *Chlamydomonas reinhardtii* upon deletion of the TLA3-CpSRP43 gene, Plant Physiol. 160 (2012) 2251–2260.
[65] C.E. Espineda, A.S. Linford, D. Devine, J.A. Brusslan, The AtCAO gene, encoding chlorophyll a oxygenase, is required for chlorophyll b synthesis in *Arabidopsis thaliana*, Proc. Natl. Acad. Sci. U. S. A. 96 (1999) 10507–10511.